Article

Near-Unity Mass Accommodation Coefficient of Organic Molecules of Varying Structure

Jan Julin,*,[†] Paul M. Winkler,[‡] Neil M. Donahue,[§] Paul E. Wagner,[‡] and Ilona Riipinen[†,§]

[†]Department of Applied Environmental Science and Bolin Centre for Climate Research, Stockholm University, SE-10691 Stockholm, Sweden

[‡]Fakultät für Physik, Universität Wien, Boltzmanngasse 5, A-1090 Wien, Austria

[§]Center for Atmospheric Particle Studies, Carnegie Mellon University, 5000 Forbes Ave, Pittsburgh, Pennsylvania 15213, United States

S *Supporting Information*

ABSTRACT: Atmospheric aerosol particles have a significant effect on global climate, air quality, and consequently human health. Condensation of organic vapors is a key process in the growth of nanometer-sized particles to climate relevant sizes. This growth is very sensitive to the mass accommodation coefficient α, a quantity describing the vapor uptake ability of the particles, but knowledge on α of atmospheric organics is lacking. In this work, we have determined α for four organic molecules with diverse structural properties: adipic acid, succinic acid, naphthalene, and nonane. The coefficients are studied using molecular dynamics simulations, complemented with expansion chamber measurements. Our results are consistent with $\alpha = 1$ (indicating nearly perfect accommodation), regardless of the molecular structural properties, the phase state of the bulk condensed phase, or surface curvature. The results highlight the need for experimental techniques capable of resolving the internal structure of nanoparticles to better constrain the accommodation of atmospheric organics.
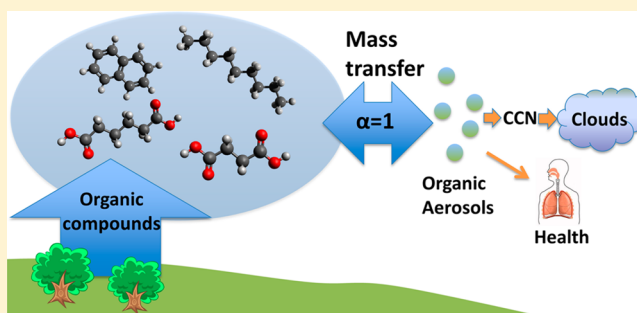
INTRODUCTION

Atmospheric aerosol particles affect air quality and human health and have an important role in defining the global climate through scattering solar radiation and through serving as cloud condensation nuclei (CCN). Many atmospheric particles are formed by nucleation, but to act as CCN, they must first grow substantially, to roughly diameters of 50−100 nm. Especially for the smallest particles, which have high Brownian diffusivity, to grow slowly is to die by collision with larger particles. Growth rates thus govern the number of climate relevant particles.[1−3]

Organic species constitute up to 90% of the atmospheric aerosol mass concentration in the submicron size range,[4] with the majority of this organic mass being secondary organic aerosol (SOA) formed in the atmosphere. The condensation of organic vapors on existing aerosol particles is a significant contributor to the growth to CCN sizes of the newly formed particles,[5,6] and proper description of the growth process is vital in order for models to be able to achieve correct CCN concentrations. The vapor uptake ability of the aerosols is described by the mass accommodation coefficient α, which is defined as the fraction of the incoming vapor molecules that remain with the condensed phase.[7] The mass accommodation coefficient affects the SOA vapor−particle equilibration time scale, which will determine whether the SOA can be modeled by assuming instant equilibration between vapor and particle

phases or if the situation should be treated as a kinetically limited process.[5,8,9] The mass accommodation coefficient needs to be well constrained for accurate modeling of SOA.[10]

In part due to the large number of organic species in the atmosphere,[11,12] the properties of the various organic species are in general poorly constrained.[13] The mass accommodation coefficient is no exception and, in fact, is even more poorly constrained than most thermodynamic properties. Though some pioneering work studying the mass accommodation coefficients of organics has been reported recently,[14−16] it has been shown that the values of the coefficient are challenging to quantify experimentally.[17] This difficulty is not limited to organics. Even the reported values for water vary by several orders of magnitude,[18−20] although recent sensitivity studies have managed to constrain the value somewhat.[17,21] Because the sheer number of atmospheric organic species makes it unfeasible to study each of them with the same level of effort that has been given to water over the years, the ability to constrain the influence of common molecular structural features on α is critical.

The mass accommodation coefficient α can be defined as either surface (α_s) or bulk accommodation coefficient (α_b).[7] The difference between the two is whether a condensing molecule needs to be absorbed to the particle bulk (bulk accommodation) for it to be considered accommodated or if it is sufficient to consider surface adsorption. Experimental studies often measure the evaporation coefficient,[14,16] and as the net evaporation and condensation fluxes are equal in equilibrium, the evaporation coefficient can be equated with the condensation, or mass accommodation, coefficient. Traditional aerosol dynamic models, which are used to interpret the experimental results, do not make any distinction between particle surface and bulk. Consequently, it is not clear whether the experimental α is a surface or bulk accommodation coefficient. Molecular level methods such as molecular dynamics (MD) simulations are able to distinguish between surface and bulk and, therefore, are essential in elucidating the nature of the mass accommodation coefficient.[22−27]

The phase of the aerosol particles can have a considerable effect on the magnitude of the coefficient. The rapid equilibration between gas and particle phases is a reasonable assumption when the particle phase is liquid,[8] although if particle-phase chemistry plays an important role, the condensational growth should still be modeled as a kinetically limited process.[28] In recent years, there has also been increasing evidence suggesting the existence of solid or semisolid (glassy) SOA particles.[14,15,29−31] This could cause kinetic limitations in the particle phase transport,[8] resulting in an apparent $\alpha < 1$. The matter is far from settled, especially as contrasting results concluding short equilibration time-scales and supporting the rapid equilibrium approach have emerged recently.[9,32] In any case, the value of the accommodation coefficient has also a major impact on the equilibration time scales of both liquid and semisolid particles.[8]

In this work, we determine the mass accommodation coefficients of selected organic molecules using MD simulations and expansion chamber measurements. The molecular species include adipic and succinic acid, which are dicarboxylic acids with different aliphatic chain length, as well as naphthalene, a simple polycyclic aromatic hydrocarbon, and n-nonane, a linear alkane. The varying structure of these molecules enables us to shed light on the effect of molecular structural properties on α. Furthermore, we distinguish between bulk and surface accommodation and constrain how the condensed phase state affects these processes. By employing both a cluster and planar target surface for adipic acid we confirm that surface curvature has a minimal effect on α. We discuss the nature and the apparent value of α in light of our results and the implications of our findings to experimentally determining the mass accommodation coefficient.

■ METHODS

Molecular-Level Definitions of α. As the molecules arrive at the surface, their fates are divided into four different possible outcomes,[24,25] which are illustrated in Figure 1: scattering, adsorption, absorption, and desorption. Of these, scattered molecules do not enter the surface at any point of their trajectory. These molecules will, for example, recoil with very high rotational quantum number in molecular beam experiments probing gas-surface collisions.[33] Molecules adsorbed to the surface can be either desorbed back to the vapor phase or absorbed into the bulk condensed phase. Using this
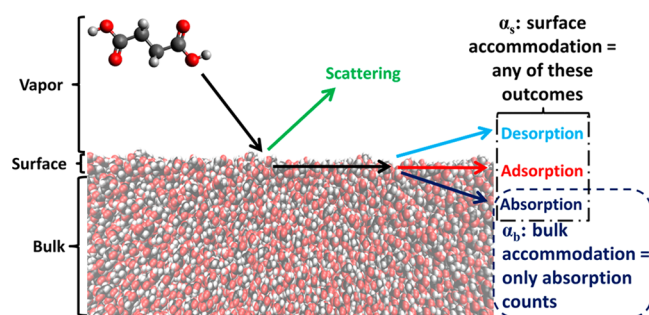

Figure 1. Schematic representation of the possible fates of an incoming molecule and of the difference between surface and bulk accommodation.

classification the surface accommodation coefficient is defined as[24]

$$\alpha_s = \frac{n_{absorb} + n_{desorb} + n_{adsorb}}{n_{total}} \tag{1}$$

where n_{absorb}, n_{desorb}, and n_{adsorb} are the number of absorbed, desorbed, and adsorbed molecules, respectively, and n_{total} is the total number of incoming molecules. The bulk accommodation coefficient is defined as

$$\alpha_b = \frac{n_{absorb} + p_k n_{adsorb}}{n_{total}} \tag{2}$$

where the correction factor p_k

$$p_k = \frac{n_{absorb}}{n_{absorb} + n_{desorb}} \tag{3}$$

is introduced because the final fate of the adsorbed molecules cannot be determined during the limited simulation time. The distinction between absorbed and adsorbed molecules will naturally depend on the chosen location of the boundary between surface and bulk. It should be noted that by adopting this terminology, we use desorption only as a possible outcome for incoming molecules. Thermal evaporation of the condensed phase molecules can occur during the simulations, and in the following, we call this simply evaporation. Generally, in terms of mass accommodation, it should not matter if it is the incoming molecule that returns to the vapor phase or if the collision causes a surface molecule to evaporate.

In this paper, we use eq 1 as the definition for the surface accommodation coefficient. The upper limit of the bulk accommodation coefficient reported in the following corresponds to the standard definition given by eq 2. However, we also report a conservative lower limit for α_b, which corresponds to eq 2 with p_k set to zero. In other words, we conservatively assume that none of the molecules classified as adsorbed will ever enter the bulk, and thus, we count only the absorbed molecules already within the bulk at the end of the simulation.

Molecular Dynamics Simulations. All simulations were performed with the Gromacs MD software,[34] and the molecules were modeled using the nonpolarizable OPLS-AA force-field,[35] with a 1.1 nm cutoff for the van der Waals interactions and the long-range part of the Coulombic interactions treated by particle-mesh Ewald summation. All bond lengths were constrained with the LINCS algorithm. A 1 fs simulation time step was used. The condensed phase was kept in constant temperature by the Bussi thermostat,[36] whereas the incoming molecules were not coupled to the

thermostat in order to avoid interfering with the accommodation process. Periodic boundaries were applied in all directions.

The different molecules and the various target surfaces are illustrated in Figure 2. The target surfaces always consisted of
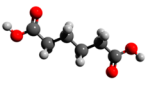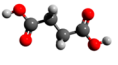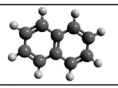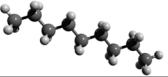
Molecule		Target surface
Adipic acid		Planar solid/semi-solid
		Cluster, diameter=5.2 nm
Succinic acid		Planar solid/semi-solid
Naphthalene		Planar subcooled liquid
Nonane		Planar liquid

Figure 2. List of the organic molecules simulated in this work and the corresponding target surfaces.

the same molecular species as the incoming molecules, and 100 incident molecules were simulated for each surface. An experimental mass accommodation coefficient has been reported for adipic acid[16,37] and succinic acid.[37] The simulation temperature for the dicarboxylic acids and naphthalene was T = 313.15 K, matching the thermodenuder temperature of Saleh et al.[16,37] This temperature is well below the melting temperature of both adipic and succinic acid and somewhat below the melting temperature of naphthalene. However, the simulated naphthalene exhibits clearly liquidlike behavior, and thus, the naphthalene condensed phase here is a subcooled liquid. The simulated dicarboxylic acids on the other hand exhibit a solid structure. There is no evidence that after the freezing and equilibration procedure described below the system would remain in an intermediate state. One should keep in mind, however, that it cannot be stated with certainty that the system would not reconfigure to some final structure if notably longer simulation times were accessible. Consequently, we indicate in Figure 2 and Table 1 that the dicarboxylic acids are either in a semisolid or solid phase. For brevity, and as opposed to the condensed phase being liquid, we refer to the dicarboxylic acid condensed phase as solid in the following. Nonane accommodation was simulated at a lower temperature of T = 280 K, matching the temperature of the nonane experiments we also report in this work. Nonane is liquid at this temperature.

The initial setup for a planar interface simulation was a liquid or solid slab of 1000 molecules in the center of a simulation box elongated in the z direction. For adipic acid a 400-molecule cluster in the center of a cubic simulation box was also simulated. An incoming molecule with random orientation was placed at about 2 nm above the surface at random x and y coordinates (for the molecule center of mass), and in the cluster case, a random z coordinate was chosen as well. The velocity of the molecule was drawn from the Maxwell−Boltzmann distribution corresponding to the temperature in question, with the requirement that the velocity vector be pointing toward the surface. Because the slab system provides two independent surfaces, an incoming molecule was placed on both sides of the slab.[23,27] Each individual simulation was run for 80 ps.

To control the effect of the angle of approach for the cluster case, the angles were constrained to two distinct cases with 100 incoming molecules for each. For the first case, the molecules were aimed directly toward the center of mass of the cluster ("direct hit"). For the second case, the "target" was a random point on a circle with 1.5 nm radius, with the center of the circle at the cluster center of mass, and the plane of the circle perpendicular to the vector between the centers of mass of the cluster and the incoming molecule ("non-direct hit", for schematic illustration see Supporting Information).

As the mass accommodation simulation temperature is below the melting points of adipic acid, succinic acid, and naphthalene, the systems were initially equilibrated in a cubic simulation box for 1 ns at a higher temperature: 460 K for succinic acid, 425 K for adipic acid, and 360 K for naphthalene, near their respective experimental melting temperatures. After this, the systems were cooled to 313.15 K by simulated annealing over 1 ns. The system is further allowed to equilibrate for several nanoseconds in the elongated box before collecting the starting configurations for the mass accommodation runs. For nonane, the initial equilibration is already performed at the desired simulation temperature, T = 280 K. For all cases, the starting configurations for the mass accommodation simulations are collected at 20 ps intervals from the slab-only (or cluster-only) runs after the equilibration procedures.

Experiment. Condensational growth of nonane was measured in an expansion chamber, the Size Analyzing Nuclei Counter (SANC),[19,38,39] using constant angle Mie scattering for the size-detection,[40] at temperature T = 280 K and total pressure p = 792.9 hPa. The liquid droplets were formed by heterogeneous nucleation of nonane vapor on Ag seed particles. A nonane−air vapor mixture was obtained with the spray-

Table 1. Simulated Surface Accommodation Coefficients According to Equation 1 and Restrictions for the Value of the Bulk Accommodation Coefficient

molecule	target surface	$\alpha_s{}^a$	$\alpha_b{}^a$
adipic acid	planar, solid/semisolid	$0.96 \leq \alpha_s \leq 1$	$0.25 \leq \alpha_b \leq 1$
	cluster, direct hit	$0.96 \leq \alpha_s \leq 1$	$0.14 \leq \alpha_b \leq 1$
	cluster, nondirect hit	$0.96 \leq \alpha_s \leq 1$	$0.19 \leq \alpha_b \leq 1$
succinic acid	solid/semi-solid	$0.96 \leq \alpha_s \leq 1$	$0.22 \leq \alpha_b \leq 1$
naphthalene	subcooled liquid	$0.96 \leq \alpha_s \leq 1$	$0.76 \leq \alpha_b \leq 1$
nonane	liquid	$0.96 \leq \alpha_s \leq 1$	$\sim0.5^b \leq \alpha_b \leq 1$

^{a}The lower limits for both α_s and α_b correspond to binomial 95% confidence intervals. The results on the accommodation of nonane are a combination of molecular dynamics simulations and experimental data. ^{b}Based on the experimental data only and depends on saturation vapor pressure used.

evaporation technique,[41] and during a measurement cycle, the vapor—air mixture was passed together with the Ag-aerosol into the expansion chamber. The expansion time in the current experiment was 10 ms. After the expansion the supersaturated vapor nucleates on the aerosol particles, and these droplets then grow by condensation to optically detectable sizes. The particle concentration and size as a function of time was measured using constant angle Mie scattering.[40]

■ RESULTS AND DISCUSSION

The surface and bulk accommodation coefficients are given in Table 1. We observed no direct scattering of incoming molecules for any of the studied molecular species or target surfaces, meaning that the surface accommodation coefficient is unity for all cases. As the resulting fate of an individual molecule can be considered a binomial variable (accommodation/nonaccommodation), we report α_s with the 95% binomial confidence interval.

The upper limit given for the bulk accommodation coefficient follows directly from the expression given by eq 2. For all of the studied molecules, this upper limit is unity, as no desorption events were observed. Table 1 shows the conservative estimate (again corresponding to the 95% binomial confidence interval) for the lower limit of the bulk accommodation coefficient, which we obtained by assuming zero p_k in eq 2. The transport from surface to bulk is slow compared to the simulation time for the current set of molecules under these conditions, and consequently, the majority of the incoming molecules remain adsorbed at the end of the simulation, with naphthalene being the only exception.

Experimental evaporation coefficients for dicarboxylic acids have previously been determined from measurements of the evaporation of aerosols in thermodenuders at $T = 40$ °C:[16,37] for adipic acid, $\alpha = 0.16 \pm 0.03$;[16] for succinic acid, $\alpha = 0.07 \pm 0.02$.[37] A correction applied to the Knudsen number should increase the latter value by 30%.[16] Although the lower-limit MD α_b could be in agreement with the experimental values, it should be kept in mind that this is a very conservative estimate. Moreover, as an incoming molecule remains on the surface longer, it will have more time to lose any excess kinetic energy and, consequently, it will be less likely to desorb. Therefore, the lower limit α_b listed in Table 1 are less likely than larger values of α_b. Thus, the agreement between experiment and simulations is tenuous.

The lower limits for α_b given in Table 1 are determined by placing the boundary between surface and bulk to where the density is 90% of the bulk condensed phase value. This means that a molecule is classified as absorbed if its center of mass has crossed this surface/bulk boundary. Although this surface definition is commonly used in MD,[24,42] it is arbitrary. Consequently, we examined the sensitivity of our derived bulk accommodation coefficient to this threshold value. Figure 3 shows how the α_b lower limit will change when the location of the surface/bulk boundary is chosen as different fraction of the bulk density, ranging from 5% to 99%. Decreasing the threshold bulk density fraction means that the location of the boundary gets closer to the vapor phase (see the Supporting Information), and accordingly, the lower limit of α_b approaches unity. It is notable that a slight change from the conventional 90% bulk density surface/bulk threshold can change the fraction of molecules classified as absorbed by a factor of 2. This slight change (going from 90% to either 80% or 95%)
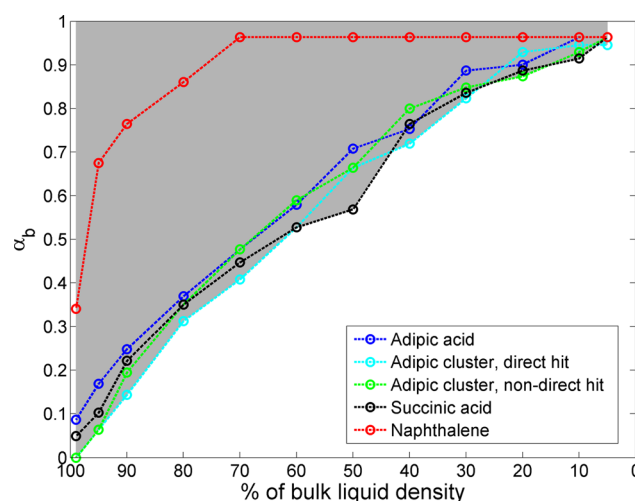

Figure 3. Conservative estimates for the lower limit of the bulk accommodation coefficient. The bulk accommodation coefficients are given as a function of the fraction of bulk condensed phase density where the boundary between surface and bulk is placed. For all cases the upper limit is unity, which is reflected by the shaded area. Direct hit refers to simulations where the incoming molecules are aimed at the cluster center of mass.

moves the location of the surface/bulk boundary by as little as 0.3 Å for most of the present cases. The results highlight the fact that the value of α_b is strongly dependent on how the condensed phase is in practice separated into the distinct surface and bulk phases. In general, the gradients shown in Figure 3 suggest steady diffusion by adsorbed molecules into the bulk; as can be expected from the slower transport from the surface to bulk when the condensed phase is a solid, the solid dicarboxylic acid surfaces result in lower possible values than the liquid naphthalene surface.

Results for adipic acid suggest that there is little if any difference between planar surfaces and small clusters, in agreement with results for liquid water.[43] Changing the angle of incidence from head-on collision to the closer-to-tangential angle of incidence had no discernible effect on α_s or α_b. The minimum α_b values are similar for planar and cluster cases, with one exception: when a high fraction of the bulk density is used to define the surface/bulk boundary, the number of molecules entering the bulk of the cluster gets notably smaller than for the corresponding planar surface. This is likely because the surface area to bulk volume ratio is over three times higher for the relatively small cluster than for the planar slab.

Unlike the other molecules studied here, nonane exhibits a distinct surface structure: a surface monolayer of molecules is arranged in the direction of the surface normal, and below this, the bulk molecules are randomly oriented. As a result, the nonane density profile shows a surface peak followed by a valley at the bulk end of the monolayer, and only below this can the region of bulk density be found (see the Supporting Information). Consequently, using a surface definition based on some fraction of the bulk liquid density makes little sense for nonane, and instead, simply taking this monolayer to be the surface is a more sensible definition. The tightly packed surface structure prevents the incoming molecules from passing through the surface monolayer within the simulation time scale, or even from taking a place within this structure. Thus, through simulation alone, we cannot restrict the nonane α_b without resorting to surface definitions ill-suited to the task. It

is worth noting that even for nonane, we observed no scattering or desorption of incoming molecules.

To constrain α_b for nonane, we use the experimental data on condensational growth of nonane droplets in an expansion chamber, illustrated in Figure 4. The experimental method is
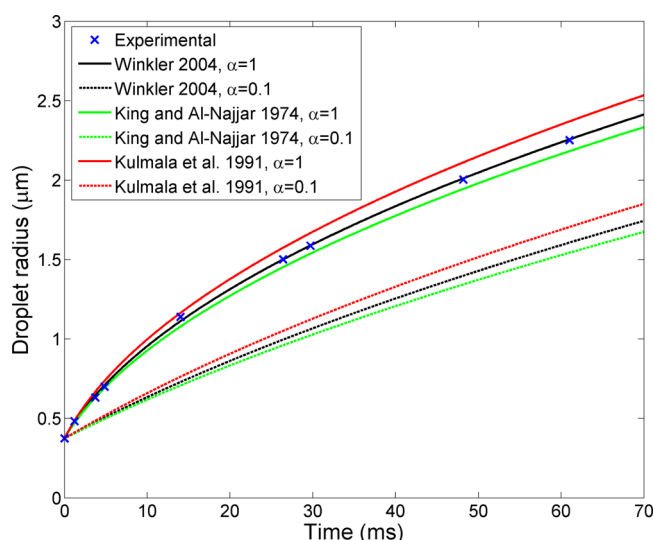

Figure 4. Condensational growth of nonane. Experimental data is denoted by crosses, the lines correspond to the different saturation vapor pressure parametrizations with solid lines having $\alpha = 1$, and the dashed lines $\alpha = 0.1$. Unity mass accommodation coefficient works better than 0.1, regardless of the saturation vapor pressure used.

the same that was used for water in ref 20 It was found by Miles et al.[17] to be the most reliable of all the analyzed experimental techniques in determining the value of α, at least in the case of water. The observed growth was modeled by solving the mass and heat transfer equations for a monodisperse, single-component aerosol population in an inert gas (see, e.g., refs 44 and 45 and the Supporting Information). The mass accommodation coefficient enters the equations through the Fuchs–Sutugin correction factor multiplying the mass flux.

In addition to the mass accommodation coefficient, the main sensitivity of the modeled growth is to the saturation vapor pressure. Figure 4 shows modeled growth curves for three different saturation vapor pressure parametrizations[46−48] and mass accommodation coefficient values 1 and 0.1. It should be noted, however, that the Winkler parametrization[48] is based on the data presented here assuming $\alpha = 1$. Regardless of the saturation vapor pressure parametrization we use, the experimentally observed growth agrees with an accommodation coefficient at or near unity, whereas $\alpha = 0.1$ leads to a clear underestimation of the droplet growth. Thus, the experimental data are consistent with the MD results. Here, the thermal accommodation coefficient, which gives the fraction of molecules that reach thermal equilibrium with the condensed phase, was assumed to be unity. The experimental method can be used to determine the thermal accommodation coefficient,[19] but a nonunity value would only require an even higher mass accommodation coefficient to match the observed growth.

Equation 2 does not place any restrictions on the desorption time scale of the incoming molecules. However, though a colliding molecule in a single-component system initially perturbs the near surface environment, once that environment relaxes to a condition indistinguishable from the precollision

condition, the colliding molecule must be accommodated. Thus, the accommodation can in theory be determined by the average time scale for desorption of an incoming molecule following a collision event: if desorption occurs after a longer time than thermal evaporation is on average expected to take place, the molecule is accommodated. Unfortunately, the evaporation time scale is for many cases impractically long for MD simulations. For example, for the two dicarboxylic acids it would take on average several microseconds to observe a single thermal evaporation event under the simulation conditions. In fact, only naphthalene condensed phase molecules are observed evaporating during the simulations, in total nine molecules during 8 ns of simulation time. This provides an estimate for the evaporation time scale for the simulated naphthalene under these conditions, but how this relates to the average desorption time scale of the incoming molecules remains unclear due to individual trajectories being followed only for 80 ps.

In conclusion, we have determined the mass accommodation coefficient of organic molecules of varying structure on surfaces consisting of the same molecular species. No scattering or desorption of incoming molecules was observed for any of the studied systems, regardless of the shape of the molecule, the phase (liquid or solid) of the condensed phase, or whether the target surface was planar or a droplet. Thus, we find that the surface accommodation coefficient is close to unity for all of the studied molecules, and the results are consistent with a unity bulk accommodation coefficient as well. Although the definite determination of the bulk accommodation coefficient would require longer simulation time scales, it should be stressed that the conservative lower limits for the bulk accommodation coefficient presented here are not very likely. MD has the benefit that it can, unlike the aerosol dynamic models that are traditionally used to interpret experiments, make a distinction between surface and bulk, even though the bulk mass accommodation coefficient is somewhat dependent on the surface definition. Therefore, as a future direction and a complement to molecular-level simulations, experimental techniques that are able to probe the surface and bulk separately are critical to resolve not only the value of the mass accommodation coefficient but the nature of it as well.

■ ASSOCIATED CONTENT

Ⓢ Supporting Information

An overview of the mass and heat transfer equations used for modeling the nonane droplet condensational growth, a schematic illustration on the initial setup of the cluster simulations, and the density profiles, with the naphthalene profile illustrating the locations of the various surface/bulk boundaries. This material is available free of charge via the Internet at http://pubs.acs.org.

■ AUTHOR INFORMATION

Corresponding Author

*E-mail: jan.julin@itm.su.se. Tel.: +46 8 674 7549. Fax +46 8 674 7325.

Notes

The authors declare no competing financial interest.

■ ACKNOWLEDGMENTS

■ REFERENCES

(1) Vehkamäki, H.; Riipinen, I. Thermodynamics and kinetics of atmospheric aerosol particle formation and growth. *Chem. Soc. Rev.* **2012**, *41*, 5160−5173.

(2) Kerminen, V.-M.; Kulmala, M. Analytical formulae connecting the "real" and the "apparent" nucleation rate and the nuclei number concentration for atmospheric nucleation events. *J. Aerosol Sci.* **2002**, *33* (4), 609−622.

(3) Kuang, C.; Riipinen, I.; Sihto, S.-L.; Kulmala, M.; McCormick, A. V.; McMurry, P. H. An improved criterion for new particle formation in diverse atmospheric environments. *Atmos. Chem. Phys.* **2010**, *10*, 8469−8480.

(4) Jimenez, J. L.; Canagaratna, M. R.; Donahue, N. M.; Prevot, A. S. H.; Zhang, Q.; Kroll, J. H.; DeCarlo, P. F.; Allan, J. D.; Coe, H.; Ng, N. L.; Aiken, A. C.; Docherty, K. S.; Ulbrich, I. M.; Grieshop, A. P.; Robinson, A. L.; Duplissy, J.; Smith, J. D.; Wilson, K. R.; Lanz, V. A.; Hueglin, C.; Sun, Y. L.; Tian, J.; Laaksonen, A.; Raatikainen, T.; Rautiainen, J.; Vaattovaara, P.; Ehn, M.; Kulmala, M.; Tomlinson, J. M.; Collins, D. R.; Cubison, M. J.; Dunlea, E. J.; Huffman, J. A.; Onasch, T. B.; Alfarra, M. R.; Williams, P. I.; Bower, K.; Kondo, Y.; Schneider, J.; Drewnick, F.; Borrmann, S.; Weimer, S.; Demerjian, K.; Salcedo, D.; Cottrell, L.; Griffin, R.; Takami, A.; Miyoshi, T.; Hatakeyama, S.; Shimono, A.; Sun, J. Y.; Zhang, Y. M.; Dzepina, K.; Kimmel, J. R.; Sueper, D.; Jayne, J. T.; Herndon, S. C.; Trimborn, A. M.; Williams, L. R.; Wood, E. C.; Middlebrook, A. M.; Kolb, C. E.; Baltensperger, U.; Worsnop, D. R. Evolution of organic aerosols in the atmosphere. *Science* **2009**, *326*, 1525−1529.

(5) Riipinen, I.; Pierce, J. R.; Yli-Juuti, T.; Nieminen, T.; Häkkinen, S.; Ehn, M.; Junninen, H.; Lehtipalo, K.; Petäjä, T.; Slowik, J.; Chang, R.; Shantz, N. C.; Abbatt, J.; Leaitch, W. R.; Kerminen, V.-M.; Worsnop, D. R.; Pandis, S. N.; Donahue, N. M.; Kulmala, M. Organic condensation: a vital link connecting aerosol formation to cloud condensation nuclei (CCN) concentrations. *Atmos. Chem. Phys.* **2011**, *11*, 3865−3878.

(6) Riipinen, I.; Yli-Juuti, T.; Pierce, J. R.; Petäjä, T.; Worsnop, D. R.; Kulmala, M.; Donahue, N. M. The contribution of organics to atmospheric nanoparticle growth. *Nature Geosci.* **2012**, *5*, 453−458.

(7) Kolb, C. E.; Cox, R. A.; Abbatt, J. P. D.; Ammann, M.; Davis, E. J.; Donaldson, D. J.; Garrett, B. C.; George, C.; Griffiths, P. T.; Hanson, D. R.; Kulmala, M.; McFiggans, G.; Pöschl, U.; Riipinen, I.; Rossi, M. J.; Rudich, Y.; Wagner, P. E.; Winkler, P. M.; Worsnop, D. R.; O'Dowd, C. D. An overview of current issues in the uptake of atmospheric trace gases by aerosols and clouds. *Atmos. Chem. Phys.* **2010**, *10*, 10561−10605.

(8) Shiraiwa, M.; Seinfeld, J. H. Equilibration timescale of atmospheric secondary organic aerosol partitioning. *Geophys. Res. Lett.* **2012**, *39*, L24801.

(9) Saleh, R.; Donahue, N. M.; Robinson, A. L. Time scales for gas-particle partitioning equilibration of secondary organic aerosol formed from alpha-pinene ozonolysis. *Environ. Sci. Technol.* **2013**, *47* (11), 5588−5594.

(10) Cappa, C. D.; Jimenez, J. L. Quantitative estimates of the volatility of ambient organic aerosol. *Atmos. Chem. Phys.* **2010**, *10*, 5409−5424.

(11) Goldstein, A. H.; Galbally, I. E. Known and unexplored organic constituents in the Earth's atmosphere. *Environ. Sci. Technol.* **2007**, *41* (5), 1514−1521.

(12) Kroll, J. H.; Donahue, N. M.; Jimenez, J. L.; Kessler, S. H.; Canagaratna, M. R.; Wilson, K. R.; Altieri, K. E.; Mazzoleni, L. R.; Wozniak, A. S.; Bluhm, H.; Mysak, E. R.; Smith, J. D.; Kolb, C. E.; Worsnop, D. R. Carbon oxidation state as a metric for describing the chemistry of atmospheric organic aerosol. *Nat. Chem.* **2011**, *3*, 133−139.

(13) Robinson, A. L.; Donahue, N. M.; Shrivastava, M. K.; Weitkamp, E. A.; Sage, A. M.; Grieshop, A. P.; Lane, T. E.; Pierce, J. R.; Pandis, S. N. Rethinking organic aerosols: semivolatile emissions and photochemical aging. *Science* **2007**, *315*, 1259−1262.

(14) Cappa, C. D.; Wilson, K. R. Evolution of organic aerosol mass spectra upon heating: implications for OA phase and partitioning behavior. *Atmos. Chem. Phys.* **2011**, *11*, 1895−1911.

(15) Vaden, T. D.; Imre, D.; Beránek, J.; Shrivastava, M.; Zelenyuk, A. Evaporation kinetics and phase of laboratory and ambient secondary organic aerosol. *Proc. Natl. Acad. Sci. U.S.A.* **2011**, *108* (6), 2190−2195.

(16) Saleh, R.; Khlystov, A.; Shihadeh, A. Determination of evaporation coefficients of ambient and laboratory-generated semivolatile organic aerosols from phase equilibration kinetics in a thermodenuder. *Aerosol Sci. Technol.* **2012**, *46*, 22−30.

(17) Miles, R. E. H.; Reid, J. P.; Riipinen, I. Comparison of approaches for measuring the mass accommodation coefficient for the condensation of water and sensitivities to uncertainties in thermophysical properties. *J. Phys. Chem. A* **2012**, *116* (44), 10810−10825.

(18) Li, Y. Q.; Davidovits, P.; Shi, Q.; Jayne, J. T.; Kolb, C. E.; Worsnop, D. R. Mass and thermal accommodation coefficients of $H_2O(g)$ on liquid water as a function of temperature. *J. Phys. Chem. A* **2001**, *105* (47), 10627−10634.

(19) Winkler, P. M.; Vrtala, A.; Wagner, P. E.; Kulmala, M.; Lehtinen, K. E. J.; Vesala, T. Mass and thermal accommodation during gas-liquid condensation of water. *Phys. Rev. Lett.* **2004**, *93* (7), 075701.

(20) Winkler, P. M.; Vrtala, A.; Rudolf, R.; Wagner, P. E.; Riipinen, I.; Vesala, T.; Lehtinen, K. E. J.; Viisanen, Y.; Kulmala, M. Condensation of water vapor: experimental determination of mass and thermal accommodation coefficients. *J. Geophys. Res.* **2006**, *111*, D19202.

(21) Raatikainen, T.; Nenes, A.; Seinfeld, J. H.; Morales, R.; Moore, R. H.; Lathem, T. L.; Lance, S.; Padró, L. T.; Lin, J. J.; Cerully, K. M.; Bougiatioti, A.; Cozic, J.; Ruehl, C. R.; Chuang, P. Y.; Anderson, B. E.; Flagan, R. C.; Jonsson, H.; Mihalopoulos, N.; Smith, J. N. Worldwide data sets constrain the water vapor uptake coefficient in cloud formation. *Proc. Natl. Acad. Sci. U.S.A.* **2013**, *110* (10), 3760−3764.

(22) Clement, C. F.; Kulmala, M.; Vesala, T. Theoretical consideration on sticking probabilities. *J. Aerosol Sci.* **1996**, *27* (6), 869−882.

(23) Morita, A.; Sugiyama, M.; Kameda, H.; Koda, S.; Hanson, D. R. Mass accommodation coefficient of water: molecular dynamics simulation and revised analysis of droplet train/flow reactor experiment. *J. Phys. Chem. B* **2004**, *108* (26), 9111−9120.

(24) Vieceli, J.; Roeselová, M.; Potter, N.; Dang, L. X.; Garrett, B. C.; Tobias, D. J. Molecular dynamics simulations of atmospheric oxidants at the air−water interface: solvation and accommodation of OH and O_3. *J. Phys. Chem. B* **2005**, *109* (33), 15876−15892.

(25) Roeselová, M.; Jungwirth, P.; Tobias, D. J.; Gerber, R. B. Impact, trapping, and accommodation of hydroxyl radical and ozone at aqueous salt aerosol surfaces. A molecular dynamics study. *J. Phys. Chem. B* **2003**, *107* (46), 12690−12699.

(26) Takahama, S.; Russell, L. M. A molecular dynamics study of water mass accommodation on condensed phase water coated by fatty acid monolayers. *J. Geophys. Res.* **2011**, *116*, D02203.

(27) Sakaguchi, S.; Morita, A. Molecular dynamics study of water transfer at supercooled sulfuric acid solution surface covered with butanol. *J. Phys. Chem. A* **2013**, *117* (22), 4602−4610.

(28) Shiraiwa, M.; Yee, L. D.; Schilling, K. A.; Loza, C. L.; Craven, J. S.; Zuend, A.; Ziemann, P. J.; Seinfeld, J. H. Size distribution dynamics reveal particle-phase chemistry in organic aerosol formation. *Proc. Natl. Acad. Sci. U.S.A.* **2013**, *110* (29), 11746−11750.

(29) Virtanen, A.; Joutsensaari, J.; Koop, T.; Kannosto, J.; Yli-Pirilä, P.; Leskinen, J.; Mäkelä, J. M.; Holopainen, J. K.; Pöschl, U.; Kulmala, M.; Worsnop, D. R.; Laaksonen, A. An amorphous solid state of biogenic secondary organic aerosol particles. *Nature* **2010**, *467*, 824−827.

(30) Perraud, V.; Bruns, E. A.; Ezell, M. J.; Johnson, S. N.; Yu, Y.; Alexander, M. L.; Zelenyuk, A.; Imre, D.; Chang, W. L.; Dabdub, D.;

Pankow, J. F.; Finlayson-Pitts, B. J. Nonequilibrium atmospheric secondary organic aerosol formation and growth. *Proc. Natl. Acad. Sci. U.S.A.* **2012**, *109* (8), 2836−2841.

(31) Renbaum-Wolff, L.; Grayson, J. W.; Bateman, A. P.; Kuwata, M.; Sellier, M.; Murray, B. J.; Shilling, J. E.; Martin, S. T.; Bertram, A. K. Viscosity of α-pinene secondary organic material and implications for particle growth and reactivity. *Proc. Natl. Acad. Sci. U.S.A.* **2013**, *110* (20), 8014−8019.

(32) Yatavelli, R. L. N.; Stark, H.; Thompson, S. L.; Kimmel, J. R.; Cubison, M. J.; Day, D. A.; Campuzano-Jost, P.; Palm, B. B.; Hodzic, A.; Thornton, J. A.; Jayne, J. T.; Worsnop, D. R.; Jimenez, J. L. Semi-continuous measurements of gas/particle partitioning of organic acids in a ponderosa pine forest using a MOVI-HRToF-CIMS. *Atmos. Chem. Phys.* **2014**, *14*, 1527−1546.

(33) Nogueira, J. J.; Vázquez, S. A.; Mazyar, O. A.; Hase, W. L.; Perkins, B. G., Jr.; Nesbitt, D. J.; Martínez-Núñez, E. Dynamics of CO_2 scattering off a perfluorinated self-assembled monolayer. Influence of the incident collision energy, mass effects, and use of different surface models. *J. Phys. Chem. A* **2009**, *113* (16), 3850−3865.

(34) Hess, B.; Kutzner, C.; van der Spoel, D.; Lindahl, E. GROMACS 4: Algorithms for highly efficient, load-balanced, and scalable molecular simulation. *J. Chem. Theory Comput.* **2008**, *4* (3), 435−447.

(35) Jorgensen, W. L.; Maxwell, D. S.; Tirado-Rives, J. Development and testing of the OPLS all-atom force field on conformational energetics and properties of organic liquids. *J. Am. Chem. Soc.* **1996**, *118* (45), 11225−11236.

(36) Bussi, G.; Donadio, D.; Parrinello, M. Canonical sampling through velocity rescaling. *J. Chem. Phys.* **2007**, *126*, 014101.

(37) Saleh, R.; Shihadeh, A.; Khlystov, A. Determination of evaporation coefficients of semi-volatile organic aerosols using an integrated volume—tandem differential mobility analysis (IV-TDMA) method. *J. Aerosol Sci.* **2009**, *40* (12), 1019−1029.

(38) Rudolf, R.; Vrtala, A.; Kulmala, M.; Vesala, T.; Viisanen, Y.; Wagner, P. E. Experimental study of sticking probabilities for condensation of nitric acid—water vapor mixtures. *J. Aerosol Sci.* **2001**, *32* (7), 913−932.

(39) Wagner, P. E.; Kaller, D.; Vrtala, A.; Lauri, A.; Kulmala, M.; Laaksonen, A. Nucleation probability in binary heterogeneous nucleation of water−n-propanol vapor mixtures on insoluble and soluble nanoparticles. *Phys. Rev. E* **2003**, *67* (2), 021605.

(40) Wagner, P. E. A constant-angle Mie scattering method (CAMS) for investigation of particle formation processes. *J. Colloid Interface Sci.* **1985**, *105* (2), 456−467.

(41) Winkler, P. M.; Hienola, A.; Steiner, G.; Hill, G.; Vrtala, A.; Reischl, G. P.; Kulmala, M.; Wagner, P. E. Effects of seed particle size and composition on heterogeneous nucleation of n-nonane. *Atmos. Res.* **2008**, *90* (2−4), 187−194.

(42) Garrett, B. C.; Schenter, G. K.; Morita, A. Molecular simulations of the transport of molecules across the liquid/vapor interface of water. *Chem. Rev.* **2006**, *106* (4), 1355−1374.

(43) Julin, J.; Shiraiwa, M.; Miles, R. E. H.; Reid, J. P.; Pöschl, U.; Riipinen, I. Mass accommodation of water: Bridging the gap between molecular dynamics simulations and kinetic condensation models. *J. Phys. Chem. A* **2013**, *117* (2), 410−420.

(44) Kulmala, M.; Vesala, T. Condensation in the continuum regime. *J. Aerosol Sci.* **1991**, *22* (3), 337−346.

(45) Vesala, T.; Kulmala, M.; Rudolf, R.; Vrtala, A.; Wagner, P. E. Models for condensational growth and evaporation of binary aerosol particles. *J. Aerosol Sci.* **1997**, *28* (4), 565−598.

(46) King, M. B.; Al-Najjar, H. A method for correlating and extending vapour pressure data to lower temperatures using thermal data: Vapour pressure equations for some n-alkanes at temperatures below the normal boiling point. *Chem. Eng. Sci.* **1974**, *29* (4), 1003−1011.

(47) Kulmala, M.; Vesala, T.; Kalkkinen, J. Data for phase transitions in aerosol systems. *Manuscript for laboratory use*; University of Helsinki: Helsinki, Finland, 1991.

(48) Winkler, P. M. *Experimental study of condensation processes in systems of water and organic vapors employing an expansion chamber.* Ph.D. Thesis, Universität Wien, 2004.